

Optical spectrum of distant OH/IR star V1648 Aql (IRAS 19386+0155)

V.G. Klochkova and N.S. Tavolzhanskaya
e-mail: valenta@sao.ru

Special Astrophysical Observatory RAS, Nizhnij Arkhyz, 369167 Russia

August 15, 2019

Abstract An optical spectrum of the star V1648 Aql (= IRAS 19386+0155) was obtained at the 6-meter telescope with a spectral resolution of $R \geq 60\,000$. Heliocentric radial velocity measured from numerous metallic absorptions is equal to $V_r = 10.18 \pm 0.05 \text{ km s}^{-1}$ ($V_{\text{LSR}} = 18.1 \text{ km s}^{-1}$). We determined the atmospheric, circumstellar, and interstellar components in the profile of the Na I D lines at $V_r = 9.2, -3.4,$ and -12.8 km s^{-1} respectively. The averaged over twenty identified DIBs velocity $V_r(\text{DIBs}) = -12.5 \pm 0.2 \text{ km s}^{-1}$ coincides with the interstellar Na I component. Weak emissions with an intensity of about 10% of the local continuum level were detected in the spectrum; they are identified as low-excitation metal lines. Their averaged position, $V_r = 8.44 \pm 0.28 \text{ km s}^{-1}$, may point to the presence of a weak velocity gradient in the upper layers of the stellar atmosphere. Based on the spectroscopic data and taking into account the interstellar and circumstellar reddening, we estimated the star's luminosity $M_V \approx -5^m$ and also obtained the lower estimate of distance $d \geq 1.8$ kpc. Using the model atmosphere method, we determined the fundamental parameters and chemical abundances in the atmosphere approving the status of a post-AGB star for V1648 Aql.

Key words. stars: evolution—stars: individual: V1648 Aql—stars: AGB and post-AGB

1. Introduction

Based on the photometric observations in the visible and IR ranges, the authors of [1] have concluded the belonging of a point infrared IRAS 19386+0155 source to the objects near the asymptotic giant branch (AGB). Despite a significant IR flux, there is no OH maser emission in the 1612-MHz band [2] which indicates a later post-AGB stage. The re-analysis of the Arecibo Observatory survey data made it possible to detect a weak radiation of the IRAS 19386+0155 source in the OH maser bands [2]. Based on the near IR polarimetry, Gledhill [4] suspected a possible belonging of IRAS 19386+0155 to bipolar nebulae.

At the post-AGB stage, far-evolved stars with initial masses within the interval of $2\div 8M_{\odot}$ are observed. At the preceding AGB stage, these stars are observed as red supergiants with effective temperature is $T_{\text{eff}} \approx 3000 \div 4500$ K. For the stars of the above masses the AGB stage is the final evolutionary stage with nuclear burning in their interiors [5]. The interest to AGB stars and their closest descendants can be explained primarily by the fact that namely in the interiors of these stars, being at a short evolutionary stage, physical conditions are created for the nuclear synthesis and ejection of the products of nuclear reactions into the stellar atmosphere and further into the circumstellar and interstellar medium. Thus, AGB stars of initial masses smaller than $3\div 4M_{\odot}$ are the main sources of heavy metals (over 50% of all the elements heavier than iron) synthesized as a result of the *s*-process, the essence of which is a slow (compared to β decay) neutronization of nuclei. A seed nucleus for a series of reactions in the *s*-process is the Fe nucleus. For stars with initial masses smaller than $3\div 4M_{\odot}$, the required neutron flux is provided by the $^{13}\text{C}(\alpha, n)^{16}\text{O}$ reaction, while in the case of more massive stars with initial masses greater than $4\div 5M_{\odot}$, a similar reaction takes place with the ^{22}Ne nuclei. These more massive AGB stars can be the sources of lithium. The evolutionary features of stars near the AGB and results of the current calculations of synthesis and ejection of elements are given in the papers [6–8].

In the visible range, the IRAS 19386+0155 source is associated with the supergiant V1648 Aql of the F5 I spectral type [9]. This supergiant is located outside the Galaxy plane that already indicates its possible belonging to the evolved stars with initial masses of $2\div 8 M_{\odot}$. To date, the star was studied by photometric methods mainly. In particular, Arkhipova et al. [10], having conducted a 19 year long *UBV* monitoring of the star, studied the light curve and revealed a sinusoidal brightness variability with an amplitude typical of post-AGB stars and an about 100^d period. Let us notice a complex character of the long-term variability of color indices of V1648 Aql detected by these authors, interpretation of which requires a further monitoring of the star. Later, Hrivnak et al. [11], having added a lot of photometric data obtained by other authors including [10] to their own observations, confirmed the periods of brightness variability and trends in the brightness and color index variabilities. V887 Her, the central star of the IR source IRAS 18095+2704, is close to V1648 Aql by the set of observed parameters. Based on the two-peaked energy distribution and a presence of OH maser radiation, Hrivnak et al. [12] consider IRAS 18095+2704 as a prototype of O-rich protoplanetary nebulae. Lewis [3], analyzing the properties of a broad sample of high-latitude OH/IR stars, also emphasized the similarity of the evolutionary state of the protoplanetary nebulae IRAS 18095+2704 and IRAS 19386+0155.

Being rather faint in the visible range, the star V1648 Aql was very rarely studied via optical spectroscopy. Pereira et al., in their paper [13] modeled the stellar atmosphere using a high-resolution spectrum in a wide wavelength range and determined the fundamental parameters and chemical abundance of the central star of this source. The authors concluded that V1648 Aql is an O-rich star with an effective temperature $T_{\text{eff}} = 6800 \pm 100$ K, the surface gravity $\log g = 1.4 \pm 0.2$, and a low metallicity $[\text{Fe}/\text{H}]_{\odot} = -1.1$. They also estimated the abundances of a number of light metals and heavy elements in the atmosphere. An important result of study [13] is modeling of an unusual for post-AGB stars energy distribution in the stellar spectrum, which allowed the authors to conclude on a possible presence of a

dust disk around the object. Unfortunately, these authors paid little attention to the features of the optical spectrum, and the paper neither has any data on the radial velocity pattern in the system at all. Thus, the need to continue the study of the system IRAS 19386+0155 is obvious.

In this paper, we present an analysis of the optical spectrum of V1648 Aql obtained in 2017. Section 2 briefly describes the methods of observations and data analysis. In Section 3, we present our results compared to those published earlier, and Section 4 gives the conclusions.

2. Observations, reduction and analysis of the spectra

The spectrum of V1648 Aql was obtained on August 7, 2017 with the NES echelle spectrograph [14] permanently mounted at the Nasmyth focus of the 6-m BTA telescope of the Special Astrophysical Observatory of the Russian Academy of Sciences. At this date, the NES echelle spectrograph was equipped with a 4608×2048 elements CCD detector with a pixel size of 0.0135×0.0135 mm and readout noise of $1.8 e^-$. The registered spectral range is $\Delta\lambda = 470\text{--}778$ nm. In order to reduce the light loss without any spectral resolution decrease, the NES spectrograph is equipped with a three-slice image slicer. Each spectral order in a 2D image of the spectrum is repeated thrice, being shifted along the echelle-grating dispersion [14]. The spectral resolution is $\lambda/\Delta\lambda \geq 60\,000$, the signal-to-noise ratio is $S/N > 100$, varying along the echelle order from 100 to 150.

Table 1. Heliocentric velocity V_r measured in the spectrum of V1648 Aql obtained on August 7, 2017. The number of measured lines of each type is given in parentheses

Lines or an element	$V_r, \text{ km s}^{-1}$		
	stellar atmosphere	CS	IS
Absorptions	10.18 ± 0.05 (349)		
Emissions	8.44 ± 0.28 (18)		
H α (core)	9.2		
H β (core)	10.6		
Na I	9.2 (2)	−3.4 (2)	−12.8 (2)
K I		−3.7 (1)	
DIBs			-12.5 ± 0.2 (20)

One-dimensional data were extracted from the 2D echelle spectra with the modified (taking into account the features of the echelle frames of the spectrograph used) ESO MIDAS reduction system ECHELLE context (see the details in paper [15]). Cosmic ray traces removal was made by the median averaging of two spectra successively obtained one after the other. Wavelength calibration was carried out using spectra of the Th–Ar hollow-cathode lamp. Further reduction including the photometric and positional measurements was performed with the latest version of the DECH20t code [16]. Note that this program code we traditionally use to reduce the spectra allows us to measure the radial velocities for separate features of line profiles. Systematic heliocentric velocity V_r measurement errors, estimated from sharp interstellar components of Na I lines do not exceed 0.25 km s^{-1} (from a single line), mean random errors for shallow absorptions are of about 0.5 km s^{-1} per line. Thus, for our

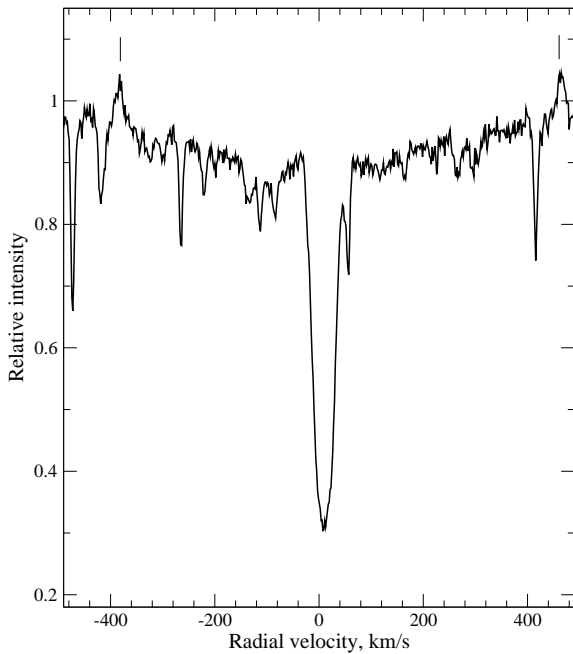


Figure 1. $H\alpha$ profile in the spectrum of V1648 Aql. The vertical lines show the positions of Ti I 6554.23 Å and Ca I 6572.80 Å emissions.

average values in Table 1, the random errors are about 0.2 km s^{-1} . We have identified the lines in the spectrum of V1648 Aql using the atlas (published earlier in [17]) of the optical spectrum of a canonical post-AGB star HD 56126 (IRAS 07134+1005, Sp=F5 Iab) based on the data observed at the 6-m telescope with the same NES spectrograph.

3. Main results

3.1. Peculiarities of the V1648 Aql spectrum and radial velocity pattern

The optical spectrum of V1648 Aql in general corresponds to the expected spectrum of an F5I supergiant meanwhile possessing several peculiarities. Firstly, the $H\alpha$ profile given in Fig. 1 in the relative intensity–radial velocity coordinates is complex and includes broad wings and a narrow core indicating a structured atmosphere of the supergiant with an envelope. Given that the $H\beta$ profile is purely absorption without any visible emission details. As it follows from Table 1, the position of the $H\beta$ core coincides with the position of atmospheric absorptions of metals. The $H\alpha$ profile in the spectrum of V1648 Aql obtained by the authors of [13] in 2000 does not differ from that we obtained almost 17 years on. This profile type is typical of post-AGB stars; Fig. 6 from [18] with the profiles in the spectra of four southern post-AGB stars can serve as an example of this.

In the spectrum of the already mentioned post-AGB-related star V887 Her, the $H\alpha$ profile demonstrated in Fig. 2 of [19] also comprises similar components. Moreover, a narrow core of this profile has envelope emissions which are less prominent in the spectrum of V1648 Aql. The same $H\alpha$ -profile type appears at certain moments of observations of HD 56126. Figure 1 in the atlas [17] gives a useful comparison of

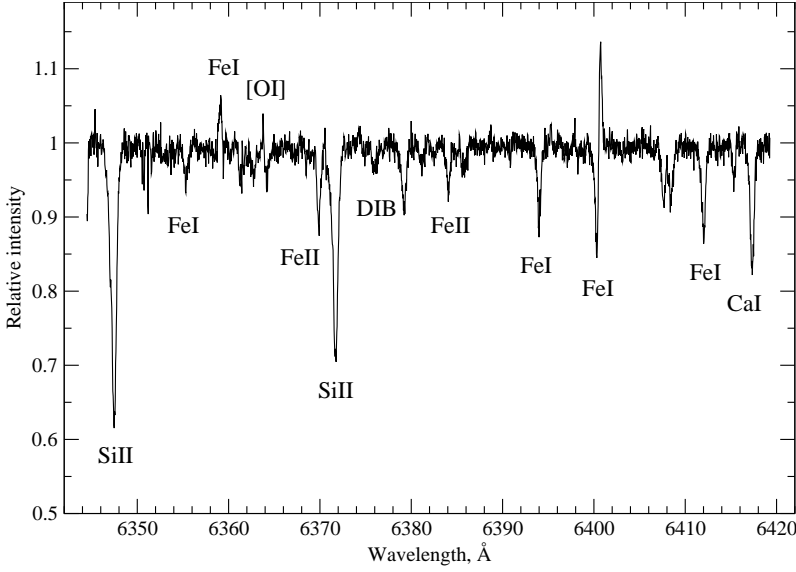


Figure 2. A fragment of the V1648 Aql spectrum containing strong Si II(2) 6347 and 6371 Å absorptions, FeI 6359 and 6400 Å emissions, an interstellar feature (DIB) $\lambda = 6376$ Å and an [OI] 6363 Å emission of ionospheric origin. The identifications of main features of the fragment are marked.

H α profiles in the spectrum of HD 56126 and in the spectrum of a classical massive supergiant α Per.

The average velocity $V_r = 10.18 \text{ km s}^{-1}$ ($V_{\text{LSR}} = 18.1 \text{ km s}^{-1}$) we have obtained from numerous metal absorptions in the spectrum of V1648 Aql proved to be in agreement with the velocity profile from OH maser bands for the associated IRAS 19386+0155 source [3] which allows us to accept the value $V_{\text{LSR}} = 18.1 \text{ km s}^{-1}$ as the systemic velocity of V1648 Aql. Note that the OH profiles for the IRAS 19386+0155 source have a large width of $\Delta V_r \approx 50 \text{ km s}^{-1}$ [3] which does not allow us to determine more accurately the value of LSR only from the radio data. Let us consider below the radial velocity pattern from special groups of spectral features identified for the first time in the V1648 Aql spectrum.

3.1.1. Metal emissions

Spectral fragment in Fig. 2 illustrates the following feature of the optical spectrum of V1648 Aql: the presence of weak emissions of neutral metals with a low excitation potential of the lower energy level. Two similar emissions in the H α wings are clearly seen in Fig. 1. Table 2 lists all the emissions of such kind we identified in the registered wavelength range. The last column of the table shows the velocity values corresponding to the emission positions. The average velocity over 18 emission features, $V_r(\text{emis}) = 8.44 \pm 0.28 \text{ km s}^{-1}$, is slightly different from the average velocity obtained from absorptions, $V_r = 10.18 \pm 0.05 \text{ km s}^{-1}$. However, taking into account a high accuracy of the average values, we can suspect a weak velocity gradient in the stellar atmosphere. Halfwidths of these emissions are about 0.3 Å, or $\Delta V_r \approx 13 \text{ km s}^{-1}$, exceeding the halfwidths of the forbidden ionospheric [OI] emissions in the spectrum by 2–2.2 times, what confirms the formation of the emissions

more likely in the atmosphere of V1648 Aql. Note that Fig. 1 from [13] also reveals emissions in the H α wings, however, the authors disregarded this feature.

Table 2. A list of metal emissions in the V1648 Aql spectrum

λ (Å)	Element	V_r , km s $^{-1}$
5644.14	TiI	11.20
5847.00	CoI	8.00
5956.70	FeI	8.78
6007.31	NiI	9.83
6108.11	NiI	10.96
6191.19	NiI	6.34
6280.62	FeI	6.57
6358.69	FeI	9.75
6498.95	FeI	8.08
6554.23	TiI	8.20
6572.80	CaI	8.41
6574.24	FeI	7.13
6624.84	VI	10.54
6743.12	TiI	9.17
7052.87	CoI	8.93
7138.91	TiI	7.21
7357.74	TiI	9.05
7714.31	NiI	9.67

Such less excited emissions of neutral metals were detected earlier [20] in the spectrum of a post-AGB candidate LN Hya (IRAS 12538–2611) having an F3 Ia spectral type similar to that of V1648 Aql. A part of the emission details of the above-mentioned type from Table 2 is present in the LN Hya spectrum too. In the case of LN Hya, the metal emissions appeared in the spectra obtained at the times of observations at its active phases in 2010, when a reverse P Cyg-type profile differed significantly from the profile observed at the quiet phases. Along with this, the position of the H α absorption component also differed considerably from that at other observation times. Moreover, the H α core was notably (by about 15 km s $^{-1}$) shifted towards the long-wave region relative to symmetric metal absorptions.

Some Fe, Co, and Ni emissions from Table 2 are also observed in the spectrum of a yellow hypergiant ρ Cas with an extended envelope (see paper [21] for details and required references). Moreover, in the ρ Cas spectrum, the average velocity from these emissions inconsiderably varies with time and differs little from the systemic velocity of the hypergiant. A small width of these emissions in the ρ Cas spectrum and an agreement of the velocity with the systemic velocity are indicative of the fact that these weak emissions form in the outer extended gaseous envelope, whose dimensions significantly exceed the photometric radius of the star. Emission lines are mainly observed in the periods when the stellar brightness decreases, which can be indicative of the relative stability of the emission intensity observed at the background of the weakened photosphere spectrum.

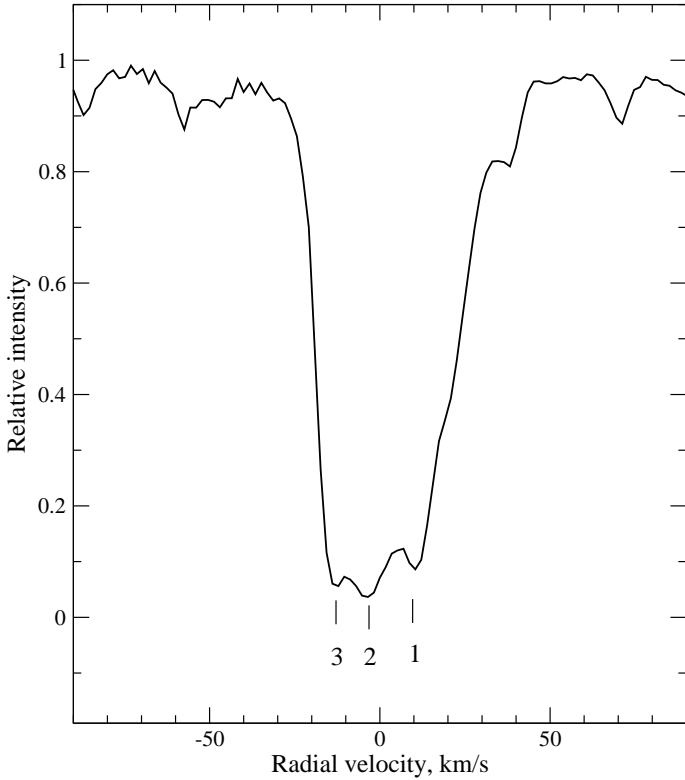


Figure 3. The Na I 5895 Å line profile in the relative intensity–radial velocity coordinates. The following positions of the profile components are marked: 1 – forms in the stellar atmosphere; 2 – forms in the circumstellar envelope, 3 – forms in the interstellar medium.

3.1.2. DIBs and a multicomponent profile of Na I D lines

The optical spectrum of V1648 Aql contains numerous interstellar features despite a considerable distance to the Galaxy plane (the galactic latitude of the star is $|b| > 10^\circ$). Table 3 presents diffuse interstellar bands (DIBs) from the well-known list of Jenniskens and Désert [22]. We have identified and reliably differentiated these DIBs among the blends in the V1648 Aql spectrum. For these features, the table lists radial velocities corresponding to band positions and their equivalent widths W_λ . The measured equivalent widths for several common DIBs agree well with the data measured in the V1648 Aql spectrum by the authors of [23]. However, radial velocities do not agree.

The high-quality spectrum allowed us to resolve into components the Na I 5889 and 5895 Å D-lines and measure the position of the interstellar KI 7696 Å absorption for the first time ever. The Na I 5889 and 5895 Å line profiles in the V1648 Aql spectrum confidently reveal individual components, the averaged position of which is given in Table 1 and in Fig. 3. The position of the long-wavelength component, $V_r = 9.2 \text{ km s}^{-1}$, complies with the average velocity V_r measured from a large selection of metal absorptions within the above error. This testifies the formation of this component in the stellar atmosphere. The location of the shortest-wavelength component of the Na I doublet lines, $V_r = -12.8 \text{ km s}^{-1}$, coincides with the average velocity $V_r(\text{DIBs}) = -12.5 \pm 0.2 \text{ km s}^{-1}$ obtained from the DIBs set identified in the

spectrum, which allows us to confirm that this component is formed in the interstellar medium. Figure 3 shows a differing steepness of wings of the atmospheric and interstellar components, which also proves our version on their formation regions.

The component of the NaI D-lines with the velocity $V_r = -3.4 \text{ km s}^{-1}$ is shifted towards the short-wavelength region by 13.6 km s^{-1} relative to the average radial velocity from the atmospheric absorptions. We can naturally suppose that this component forms in the circumstellar envelope expanding with the velocity $V_{\text{exp}} = 13.6 \text{ km s}^{-1}$ typical of post-AGB stars (see numerous examples in [24, 25] for comparison).

Table 3. DIBs parameters in the V1648 Aql spectrum

λ , Å	V_r , km s^{-1}	W_λ , mÅ
5456.00	-13.73	15
5487.67	-12.99	18
5512.68	-14.02	16
5780.48	-12.43	200
5849.81	-11.65	7
5910.57	-14.10	12
6089.85	-10.09	13
6158.57	-11.29	41:
6195.98	-14.14	40
6203.05	-12.60	88
6234.03	-11.16	22
6269.85	-13.62	33
6376.08	-13.63	19
6379.32	-13.64	55
6445.28	-11.92	6
6449.22	-14.83	7
6613.62	-12.37	144
6660.71	-12.23	28
7367.13	-12.76	28
7651.40	-13.22	15

3.1.3. Luminosity and distance to the star

The Gaia DR2 catalog gives an unreliable (negative) parallax for V1648 Aql (as well as for some other distant stars with extended dust envelopes) which already indicates a vast distance to the object. Let us try to estimate the luminosity of the star and the distance to it based on the spectroscopic data we obtained. To estimate the $E(B-V)$ color excesses determined by the interstellar extinction, we use the measured intensities for the selected DIBs and the calibrations $E(B-V) \leftrightarrow W_\lambda(\text{DIBs})$ according to the data from [26]. Using only eight mostly reliably measured bands with $W_\lambda > 10 \text{ mÅ}$ from Table 3, we obtain the average color excess of $E(B-V) = 0^{\text{m}}68$. This color excess index is caused by the interstellar extinction only. Some fraction of the complete reddening of the star is caused by the extinction not in the interstellar but rather in the circumstellar medium. Thus, it is natural that our color excess estimate is somewhat smaller than the value of $E(B-V) = 0^{\text{m}}8 - 0^{\text{m}}9$ in [10].

We will estimate the stellar luminosity using the well-known luminosity criterion for the evolved stars — the intensity of the oxygen triplet OI 7774 Å. The total equivalent width of the triplet in our spectrum equals $W_\lambda(7774)=1.42$ Å which is typical of post-AGB stars (see the data in [27] for comparison). Along with this, the equivalent width of the triplet in the V1648 Aql spectrum is $1.5\div 2$ times lower than the equivalent width of the triplet in the spectra of high-luminosity massive stars of a close spectral type, V1302 Aql [28] and V509 Cas [29]. Taking into account the calibration of $M_V \leftrightarrow W_\lambda(7774)$, according to [30], we obtain the V1648 Aql luminosity corresponding to the intensity of the triplet in the spectrum: $M_V \approx -5^m$. Results of Takeda et al. [30] allow us to notice a good agreement of two spectral parameters obtained from the V1648 Aql spectrum, namely, the surface gravity and $W_\lambda(7774)$.

The luminosity we obtained agrees well with the spectral classification and the luminosity expected from theoretical concepts on the evolution of post-AGB stars [31]. However, the luminosity estimate obtained from $W_\lambda(7774)$ is not quite accurate due to a number of reasons. Firstly, V1648 Aql shows a long-term trend of the apparent brightness at about 0^m4 [10]. Secondly, the equivalent width of the OI 7774 Å triplet can be increased due to a great oxygen overabundance in the atmosphere of V1648 Aql. Kovtyukh et al. [32] considered the influence of stellar parameters, including their metallicity on the calibration $M_V \leftrightarrow W_\lambda(7774)$. Along with this, they justly noted an inconsiderable effect of the oxygen abundance on W_λ of the strong lines of the OI 7774 Å triplet.

Taking into account the apparent brightness trend from paper [10] and the absorption value $A_V=2^m17$ (with the standard value of $R=3.2$), we obtain the distance to the star of $d\approx 5$ kpc. If we also consider the color excess due to absorption in the stellar envelope which is about 0^m4 according to Arkhipova et al. [10], then the distance to the star will decrease to 3.8 kpc (at $R=3.2$) and even to 1.8 kpc (at $R=7.4$). Here we should mention the distance estimate to IRAS 19386+0155 in the catalog [33]. Modeling the SED, these authors came to the luminosity estimate $L/L_\odot=6000$ which is close to our luminosity determination from the oxygen triplet. In this regard, they derived a small color excess $E(B-V)=0^m36$ and the distance $d=3.3$ kpc. These estimates are precarious, if we take into account an anomalous character of the SED for IRAS 19386+0155, conditioned by the presence of warm (of about 1000 K) and cold (of about 200 K) dust [13].

On the whole, we have to admit that the distance to V1648 Aql has not so far been determined precisely, although we believe its bottom estimate to be $d\approx 1.8$ kpc.

3.2. Chemical composition of the V1648 Aql atmosphere

While we estimate the chemical composition of the stellar atmosphere, it is always quite complicated to state the main parameters: the effective temperature T_{eff} and the surface gravity $\log g$. The task becomes even more complex for an object with a circumstellar dust envelope, for which it is difficult to use the photometric data in determination of an effective temperature due to an uncertain reddening. As initial parameters for the model T_{eff} , $\log g$ and microturbulent velocity ξ_t , we used the values determined for V1648 Aql with a high accuracy within the purely spectral approach [13]. These authors obtained reliable chemical element abundances based on a high-quality spectrum using a modern analysis method. We shall there-

Table 4. Chemical element abundances $\log \varepsilon(X)$ in the V1648 Aql atmosphere. The error of mean abundance σ obtained from a number of lines n is listed. The chemical composition of the solar atmosphere is taken from [37]. The last column gives the relative abundances in the atmosphere of a related star V887 Her [38].

The Sun		V1648 Aql (the present paper)					V887 Her [38]
Elm	$\log \varepsilon(E)$	X	$\log \varepsilon(X)$	σ	n	$[X/Fe]_{\odot}$	$[X/Fe]_{\odot}$
C	8.39	CI	8.47	0.10	13	+0.75	+0.43
N	7.86	NI	7.88		1	+0.69	$\leq +0.46$
O	8.73	OI	9.42	0.26	3	+1.36	+0.77
Na	6.30	NaI	6.01	0.16	4	+0.38	+0.79
Mg	7.54	MgI	7.43	0.16	3	+0.48	+0.45
Si	7.52	SiI	7.05	0.17	7	+0.20	+0.58
		SiII	7.41	0.14	2	+0.56	+0.10
S	7.14	SI	7.55	0.30	4	+1.08	+0.77
Ca	6.33	CaI	5.87	0.14	13	+0.21	+0.05
Sc	3.07	ScII	2.47	0.15	9	+0.07	-0.16
Ti	4.90	TiI	4.26	0.45	3	+0.03	-0.07
		TiII	4.26	0.14	12	+0.03	0.00
Cr	5.64	CrI	5.12	0.16	9	+0.14	-0.02
		CrII	5.14	0.09	17	+0.17	-0.19
Fe	7.45	FeI	6.77	0.04	121	-0.01	0.00
		FeII	6.80	0.09	26	+0.02	0.00
Ni	6.23	NiI	5.61	0.13	9	+0.05	+0.17
Zn	4.62	ZnI	4.02	0.27	3	+0.17	+0.21
Y	2.21	YII	1.15	0.25	4	-0.40	-0.58
Ba	2.17	BaII	1.39	0.25	4	-0.11	-0.22
Ce	1.61	CeII	0.79		1	-0.15	
Eu	0.52	EuII	0.35	0.10	3	+0.50	+0.34

fore consider below the chemical composition that we have obtained only in brief, highlighting some key points.

Endeavoring to keep the ionization balance for FeI and FeII, we performed many calculations of their abundances varying the main parameters of the atmosphere model. As final values, we accepted the following: $T_{\text{eff}}=6800\pm 100$ K, $\log g=1.2\pm 0.2$, $\xi_t=8.3\pm 0.5$ km s^{-1} which within the error agree with the parameters from [13]. The choice of the effective temperature and surface gravity is confirmed by a good agreement of abundances from absorptions of neutral atoms and ions for Ti and Cr. Herein, the agreement is worse for silicon which is of little significance owing to a small number of SiII lines. When determining the parameters of the model atmosphere and calculating the abundances, we used the lines of small and moderate intensity with the equivalent widths of $W_{\lambda} \leq 0.25$ \AA , since the approximation of the stationary plane-parallel atmosphere can be inadequate while describing the stronger spectral features. All the absorption equivalent widths are measured in the Gaussian approximation. Oscillator strengths $\log gf$ and other atomic constants are adopted from the VALD database [34, 35]. We performed the calculations of plane-parallel models and chemical abundance in the approximation of the local thermodynamic

equilibrium (LTE) using the latest version of the software designed and adapted for the OS Linux environment by V. Tsymbal [36].

Table 4 gives the obtained average element abundances $\log \varepsilon(E)$, as well as the relative abundances $[X/Fe]_{\odot}$. The chemical composition of the solar photosphere given in the second column, relative to which we consider the abundances of chemical elements of the star studied, is borrowed from [37]. The scatter of the chemical element abundances obtained from a set of lines is insignificant: the mean error σ generally does not exceed 0.3 dex for the elements with more than four absorptions used (see Table 4).

3.2.1. Iron-peak elements

The iron abundance, usually accepted as stellar metallicity, in the atmosphere of V1648 Aql differs from the solar abundance: $\lg \varepsilon(\text{FeI})=6.82$. The reliably determined abundances of titanium, chromium and nickel belonging to the iron group also differ little from normal: $(\text{Ti,Cr I,Ni})/Fe_{\odot}=+0.12$.

3.2.2. Light elements

When analyzing the characteristics of the chemical abundance of the V1648 Aql atmosphere, one should consider the results of modeling its energy distribution (SED) [13], based on which the envelope of the star is referred to the O-rich type. According to current concepts [7, 39], the presence of freshly generated lithium, whose synthesis is due to the HBB-process, can be expected in the atmosphere of an O-rich star at the post-AGB stage. The LiI 6707.8 Å line is absent in the spectrum of V1648 Aql, which is indicative of its belonging to stars with initial masses below $4 M_{\odot}$ [40].

A considerable oxygen excess is detected in the atmosphere: its relative abundance is $[O/Fe]_{\odot}=+1.36\pm 0.26$. Given a smaller carbon excess $[C/Fe]_{\odot}=+0.75\pm 0.10$, we obtain a ratio $O/C > 1$. A significant excess of oxygen is consistent with the fact that V1648 Aql is a low-mass supergiant. An analysis of the spectra of massive stars [41] shows that, in accordance with the theoretical predictions, the evolution of massive stars results in the deficiency of oxygen, which is converted into nitrogen during the CNO cycle. Therefore, nitrogen is an essential element for reliable determination of the evolutionary status of a star. In the registered spectral range, only one of its lines is available to us: NI 7468 Å. The nitrogen abundance, $[N/Fe]_{\odot}=+0.69$, is calculated based on the measured equivalent width of this rather weak line, $W_{\lambda}=22 \text{ m}\text{\AA}$. The ratio $O/N > 1$ also confirms the low-mass supergiant status of V1648 Aql.

We determined the sodium abundance from the weak subordinate NaI 5682, 5688, 6154, and 6160 Å lines, for which the corrections caused by a shift from the LTE are minimal [42]. The detected sodium excess, $[\text{NaI}/Fe]_{\odot}=+0.38\pm 0.16$, is small and does not exceed 3σ . However, taking into consideration the abundances of other metals of the α -process (Mg, Si, S, and Ca), we can speak about the presence of their small excess that is typical of unevolved stars with the metallicity of $[\text{Fe}/H]_{\odot} < -0.5$ [43].

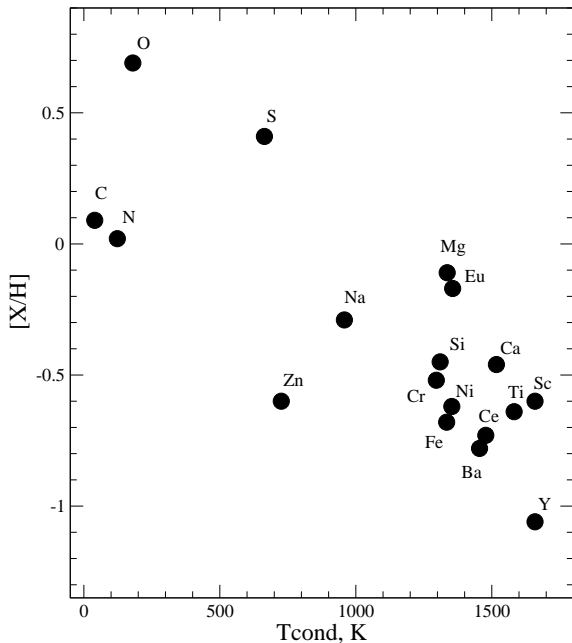


Figure 4. Abundances of chemical elements in relation to the solar ones $[X/H]_{\odot}$ in the atmosphere of V1648 Aql depending on the condensation temperature T_{cond} from [37].

3.2.3. On selective depletion of chemical elements

For stars with gas and dust envelopes, an effective mechanism that creates chemical abundance anomalies can be the selective separation of chemical elements. In the star under study with an IR flux excess, an intensive exchange of matter of the atmosphere and the circumstellar gas-and-dust envelope can occur, as V1648 Aql has an effective temperature suitable for this process [44]. In general, the analysis of chemical element abundances is complicated by the fact that the abundances of individual elements (CNO triad, heavy metals) can be influenced both by the nuclear processes during the stellar evolution and by a selective depletion of atoms on the dust particles. A possible shift from the LTE for all chemical elements given in Table 4 does not exceed 0.1 dex (see paper [44] and references therein).

The dependence of the element abundances we obtained $[X/H]$ from Table 4 on the condensation temperature T_{cond} from [37] in Fig. 4 indicates the presence of a moderate selective depletion in the V1648 Aql system. We can expect the same behavior of elements with similar values of T_{cond} . For example, according to [37], T_{cond} is similar for calcium and scandium, as well as for barium and cerium. Indeed, as follows from Table 4 and Fig. 4, these pairs of elements have similar relative abundances.

Figure 4 shows a considerable difference of the $[X/H]$ abundances for sulfur and zinc with similar values of T_{cond} . What is important in this pair of elements is the zinc abundance, which, being little susceptible to the depletion process, does not change its abundance in the course of the nuclear evolution of this star. As it was already shown in 1991 by Sneden et al. [45], in a large range of metallicities, the zinc abundance corresponds to the behavior of iron, $[Zn/Met]=+0.04$. The conclusion by Sneden et al. refined the results of Mishenina et al. [46]: according to this work,

zinc corresponds to metallicity in a wide range of its values, $[\text{Fe}/\text{H}] = -0.5 \div -3.0$. In the V1648 Aql atmosphere, the relative abundance of zinc is $[\text{Zn}/\text{Fe}] = +0.17 \pm 0.27$, which indicates a small and statistically insignificant depletion of iron atoms.

The sulfur excess, poorly susceptible to selective condensation is $[\text{X}/\text{H}] = +0.41$, and relative to iron $[\text{X}/\text{Fe}]_{\odot} = +1.08$, which is significantly higher than the abundance excesses of other α process elements. A large difference between the relative abundances of sulfur and zinc is a common phenomenon for post-AGB stars and RV Tau-type stars, which is not explained so far [44]. As Fig. 3 in [47] and Figs. 5 and 6 in a recent publication [48] demonstrate, this difference can reach an order of magnitude and greater. As follows from paper [47], a great $[\text{S}/\text{Zn}]$ ratio is typical of stars in the thick disk. The belonging of V1648 Aql to the population of the thick disk is confirmed by the magnitude of the ratio $[\text{Zn}/\text{H}]_{\odot} = -0.6$ [44].

3.2.4. Heavy metals

No excess of the s -process heavy metals (Y, Ba, and Ce) has been detected in the atmosphere of V1648 Aql. Therefore, we can speak about the inefficiency of the third dredge-up. The absence of the expected excess of heavy metals with respect to iron is a fact known for post-AGB supergiants. The deficiency of the s -process elements in the atmospheres of post-AGB stars is observed much more often than their excess [25, 49–51]. The presence or absence of an excess of the s -process elements is associated with the initial mass of a star and the mass loss rate at the AGB stage, which determine the evolution of an individual star and the mass of the stellar core [6]. The deficiency of heavy metals in the atmosphere of the star under study could have been predicted due to the belonging of IRAS 19386+0155 to O-rich sources, as an excess of s -process elements is usually associated with a carbon excess in the atmosphere of a star having a carbon-rich envelope [25]. The estimated excess of europium $[\text{X}/\text{Fe}]_{\odot} = 0.50$ synthesized mainly in the rapid neutron capture reactions (the r -process) is typical of the atmospheres of post-AGB stars (see examples in papers [18, 50, 51]).

In whole we can approve that the parameters we obtained, namely, luminosity, distance, metallicity, and the features of chemical abundance, agree with the fact that the star is at the post-AGB stage in the thick (or, taking into consideration a small velocity of the star, in the old thin) Galaxy disk.

Let us emphasize the lack of variations of stellar effective temperature from 2000 to 2017, which could be expected due to the observed increase of the apparent brightness [10]. Note that the atmospheric parameters and the main features of the chemical abundances pattern of two high-latitude post-AGB stars V1648 Aql and V887 Her [19, 38] compared in Table 4 confirm the similarity of both objects. However, they have fundamentally different distributions of energy: unlike V1648 Aql, V887 Her has a double-peaked distribution typical of post-AGB stars. In the parameter domain, similar objects also located outside the Galactic plane are LN Hya [20, 44, 47] and the central star of the IR source IRAS 18025–3906 [48].

Based on the features of the anomalous SED, the authors of [13] drew another fundamental conclusion: a possible presence of a circumstellar dust disk in the V1648 Aql system may indicate the presence of a component in the system.

Considering the anomalous brightness variability of the star too [10, 11], spectral monitoring is required in order to search for the variability of the spectrum, the velocity field, and to identify a possible binarity of the star.

4. Conclusions

Using the 6-m BTA telescope combined with the NES echelle spectrograph ($R \geq 60\,000$), we obtained the optical spectrum of V1648 Aql, the central star of the IRAS 19386+0155, which allowed us to study for the first time the kinematic state of its extended atmosphere, circumstellar envelope, and interstellar medium in the direction of the object.

The radial velocity measured from numerous metal absorptions is $V_r = 10.18 \pm 0.05 \text{ km s}^{-1}$. The velocity averaged over the set of twenty DIBs identified in the spectrum is $V_r(\text{DIBs}) = -12.5 \pm 0.2 \text{ km s}^{-1}$. In the profile of the NaID lines, three separate components are determined:

- a long-wave component, $V_r = 9.2 \text{ km s}^{-1}$, whose position coincides with the averaged position of metal absorptions, is formed in the atmosphere of the star;
- the most short-wavelength component, $V_r = -12.8 \text{ km s}^{-1}$, whose position coincides with the average velocity from a set of twenty DIBs, is formed in the interstellar medium;
- the component with the velocity $V_r = -3.4 \text{ km s}^{-1}$, shifted towards the short wavelength region by 12.6 km s^{-1} relative to the average radial velocity from atmospheric absorptions, is formed in the circumstellar envelope expanding at a velocity typical of post-AGB stars.

We detected narrow emissions in the spectrum with the intensity of about 10% of the local continuum level, which we identified with low-excited lines of metal atoms. Their position shifted relative to the absorptions, with the average value of $V_r = 8.4 \pm 0.3 \text{ km s}^{-1}$, might indicate on the presence of a weak velocity gradient in the upper atmosphere of the star.

The intensity of the oxygen triplet $\text{OI } 7773 \text{ \AA}$ corresponds to the luminosity of $M_V \approx -5^m$. In the absence of reliable parallax of the star, we obtained the bottom distance estimate $d \geq 1.8 \text{ kpc}$, taking into account the interstellar and circumstellar reddening.

Using the model atmosphere method, we determined the fundamental parameters and abundances of 18 chemical elements in the atmosphere confirming the status of a post-AGB star for V1648 Aql.

Acknowledgements. The authors thank the Russian Foundation for Basic Research for partial financial support (project 18-02-00029 a). In this study we made use of the SIMBAD, SAO/NASA ADS, VALD, and Gaia DR2 astronomical databases.

References

1. W.E.C.J. Veen, H.J. Habing, and T.R. Geballe, *Astron and Astrophys.* **226**, 108 (1989).
2. B.M. Lewis, J. Eder, and Y. Terzian, *Astrophys. J.* **362**, 634 (1990).

3. B.M. Lewis, *Astrophys. J.* **533**, 959 (2000).
4. T.M. Gledhill, *Mon. Not. R. Astron. Soc.* **356**, 883 (2005).
5. T.Blöcker, *Astron and Astrophys.* **297**, 727 (1995).
6. F. Herwig, *Ann. Rev. Astron. Astrophys.* **43**, 435 (2005).
7. M. Di Criscienzo, P. Ventura, D.A García-Hernández, et al., *Mon. Not. R. Astron. Soc.* **462**, 395 (2016).
8. N. Liu, R. Gallino, S. Bisterzo, et al., *Astrophys. J.* **865**, 112 (2018).
9. O. Suarez, P. García-Lario, A. Manchado, et al., *Astron and Astrophys.* **458**, 173 (2006).
10. V.P. Arkhipova, N.P. Ikonnikova, G.V. Komissarova, *Astron. Let.* **36**, 269 (2010).
11. B.J. Hrivnak, W. Lu, K.A. Nault, *Astron. J.* **149**, 184 (2015).
12. H.J. Hrivnak, S. Kwok, K.M. Volk, *Astrophys. J.* **331**, 832 (1988).
13. C.B. Pereira, S. Lorenz-Martins, and M. Machado, *Astron and Astrophys.* **422**, 637 (2004).
14. V.E. Panchuk, V.G. Klochkova, and M.V. Yushkin, *Astron. Rep.* **61**, 820 (2017).
15. M.V. Yushkin, V.G. Klochkova, Preprint No.206, SAO RAS (Special Astrophysical Observatory RAS, 2004).
16. G.A. Galazutdinov, Preprint No.92, SAO RAS (Special Astrophysical Observatory RAS, 1992).
17. V.G. Klochkova, E.L. Chentsov, N.S. Tavorzhanskaya, M.V. Shapovalov, *Astrophys. Bull.* **62**, 162 (2007).
18. R.E. Molina, S. Giridhar, C.B. Pereira, et al., *Revista Mex. Astron. Astrofis.* **50**, 293 (2014).
19. V.G. Klochkova, *Mon. Not. R. Astron. Soc.* **272**, 710, (1995).
20. V.G. Klochkova, V.E. Panchuk, *Astron. Rep.* **56**, 104 (2012).
21. V.G. Klochkova, V.E. Panchuk, N.S. Tavorzhanskaya, *Astron. Rep.* **62**, 623 (2018).
22. P. Jenniskens and F.X. Désert, *Astron and Astrophys. Suppl.* **106**, 39 (1994).
23. R. Luna, N.L.J. Cox, M.A. Satorre, et al., *Astron and Astrophys.* **480**, 133 (2008).
24. E. Bakker, E.F. van Dishoeck, L.B.F.M. Waters, T. Schoenmaker, *Astron and Astrophys.* **323**, 469 (1997).
25. V.G. Klochkova, *Astrophys. Bull.* **69**, 279 (2014).
26. J. Kos, T. Zwitter, *Astrophys. J.* **774**, 72 (2013).
27. R.E. Molina, *Revista Mex. Astron. Astrofis.* **54**, 397 (2018).
28. V.G. Klochkova, M.V. Yushkin, E.L. Chentsov, V.E. Panchuk, *Astron. Rep.* **46**, 139 (2002).

29. V.G. Klochkova, E.L. Chentsov, V.E. Panchuk, *Astrophys. Bull.* **74**, 41 (2019).
30. Y. Takeda, G. Jeong, and I. Han, *Publ. Astron. Soc. Japan* **70**, id.8 (2018).
31. T. Blöcker, *Astron and Astrophys.* **299**, 755 (1995).
32. V.V. Kovtyukh, N.I. Gorlova, S.I. Belik, *Mon. Not. R. Astron. Soc.* **423**, 3268 (2012).
33. S.B. Vickers, D.J. Frew, O.A. Parker, I.S. Bojicic, *Mon. Not. R. Astron. Soc.* **447**, 1673 (2015).
34. N.E. Piskunov, F. Kupka, T.A. Ryabchikova, et al., *Astron and Astrophys. Suppl.* **112**, 525 (1995).
35. F. Kupka, N.E. Piskunov, T.A. Ryabchikova, et al., *Astron and Astrophys. Suppl.* **138**, 119 (1999).
36. V.V. Tsymbal, *ASP Conf. Ser.* **108**, 198 (1996).
37. K. Lodders, in: *Principles and Perspectives in Cosmochemistry* (Springer-Verlag, Berlin, Heidelberg, 2010), p. 379 (Astrophysics and Space Science Proc.).
38. T. Sahin, D. Lambert, V.G. Klochkova, N.S. Tavganskaya, *Mon. Not. R. Astron. Soc.* **410**, 612, (2011).
39. D.A. Garcia-Hernandez, O. Zamora, A. Yagüe, et al., *Astron and Astrophys.* **555**, id.L3 (2013).
40. P. Ventura and F. D'Antona, *Astron and Astrophys.* **439**, 1075 (2005).
41. K. Venn, *Astrophys. J.* **414**, 316 (1993).
42. K. Lind, M. Asplund, P.S. Barklem, A.K. Belyaev, *Astron and Astrophys.* **528**, A103 (2011).
43. J.C. Wheeler, C. Sneden, J.W.Jr. Truran, *Ann. Rev. Astron. Astrophys.* **27**, 279 (1989).
44. S. Sumangala Rao, S. Giridhar, D.L. Lambert, *Mon. Not. R. Astron. Soc.* **419**, 1254, (2012).
45. C. Sneden, R.G. Cratton, D.A. Crocker, *Astron and Astrophys.* **246**, 354 (1991).
46. T.V. Mishenina, V.V. Kovtyukh, C.Soubiran, et al., *Astron and Astrophys.* **396**, 189 (2002).
47. Y. Takeda, H. Taguchi, K. Yoshioka, et al., *Publ. Astron. Soc. Japan* **59**, 1127 (2007).
48. R.E. Molina, C.B. Pereira, A. Arellano Ferro, *astro-ph-SR*. 1901.058 (2019).
49. V.G. Klochkova, *Bull. Spec. Astrophys.Observ.* **44**, 5 (1997).
50. H. van Winckel, M. Reyniers, *Astron and Astrophys.* **354**, 135 (2000).
51. V.G. Klochkova, V.E. Panchuk, *Astron. Rep.* **60**, 344 (2016).